DOI: 10.1002/ ((please add manuscript number))

Article type: Full Paper

Improving the property-function tuning range of thiophene materials *via* facile synthesis of oligo/polythiophene-S-oxides and mixed -S-oxides/-S,S-dioxides

Francesca Di Maria, Mattia Zangoli, Ilaria Elena Palama', Eduardo Fabiano, Alberto Zanelli, Magda Monari, Andrea Perinot, Mario Caironi, Vincenzo Maiorano, Antonio Maggiore, Marco Pugliese, Elisabetta Salatelli, Giuseppe Gigli, Ilenia Viola, Giovanna Barbarella**

We describe for the first time a platform for the facile synthesis of oligo- and polythiophene-S-oxides and the corresponding -S,S-dioxides in short times, mild conditions, high yields. Employing ultrasound assistance we were able to selectively mono- or di-oxygenate brominated thiophenes at room T. These building blocks were then combined with metalated thiophenes via microwave assisted cross coupling reactions through a "Lego-like" strategy to afford unprecedented oligo/polythiophene-S-oxides and mixed -S-oxides/-S,S-dioxides. We demonstrate that depending on the number, type and sequence alternation of non-oxygenated, mono-oxygenated and di-oxygenated thiophene units a very wide property-function tuning can be achieved spanning from frontier orbital energies and energy gaps, to charge transport characteristics and supramolecular H-bonding interactions with specific proteins inside live cells.

Dr. F. Di Maria
Dpt. of Mathematics and Physics 'Ennio De Giorgi', via Monteroni, University of Salento, I-73100 Lecce and CNR-ISOF, I-40129 Bologna, Italy
E-mail: francesca.dimaria@isof.cnr.it
Dr. M. Zangoli, Dr. A. Zanelli, Dr. G. Barbarella
CNR-ISOF and Mediteknology, Consiglio Nazionale Ricerche, Via P. Gobetti 101, I-40129 Bologna, Italy
E-mail: giovanna.barbarella@isof.cnr.it
Dr. Eduardo Fabiano
CNR-NANO (ECMT) and Center for Biomolecular Nanotechnologies@UNILE (IIT), I-73010 Arnesano, Lecce, Italy

Prof. Magda Monari
Dpt. of Chemistry Giacomo Ciamician, University of Bologna, Via Selmi 2,
I-40126 Bologna , Italy
Dr. Mario Caironi
Center for Nano Science and Technology@PoliMi, Istituto Italiano di Tecnologia, Via G. Pascoli 70/3, I-20133 Milano, Italy
Dr. Andrea Perinot
Dipartimentodi Fisica, Politecnico di Milano, Piazza Leonardo da Vinci 32,
I-20133 Milano, Italy and Center for Nano Science and Technology@PoliMi,
I-20133 Milano, Italy
Prof. Elisabetta Salatelli
Dpt. of Industrial Chemistry Toso Montanari, University of Bologna,
Viale del Risorgimento 4, I-40136 Bologna, Italy
Prof. Giuseppe Gigli, Dr. Ilaria Elena Palama', Dr. Vincenzo Maiorano, Dr. Antonio Maggiore, Dr. Marco Pugliese
CNR-NANOTEC, Via Arnesano, I-73100 Lecce, Italy
Dr. Ilenia Viola
Dpt. of Physics, La Sapienza University, Piazzale Aldo Moro 5, I-00185 Rome, Italy and CNR-NANOTEC, Via Arnesano, I-73100 Lecce, Italy

Keywords: synthesis of thiophene materials, thiophene sulfur chemoselective oxidation, oligothiophene-S-oxides, polythiophene-S-oxides, charge transport of oligo and polythiophene-S-oxides, cytotoxicity of thiophene-S-oxides, cytotoxicity of thiophene-S,S-dioxides

1. Introduction

Oligo- and polythiophenes are of outstanding importance in organic materials science and technology.[1] Numerous studies on their basic chemical and physical properties, their applications as active device components in organic electronics and bioelectronics, as selective chemosensors and biosensors for a variety of target analytes and as fluorescent reporters in bioimaging have been published. There is great current interest for their application in photovoltaic cells,[2] field-effect transistors,[3] the identification of intracellular protein aggregates associated with Alzheimer's disease,[4] and as effective membrane probes with high mechanosensitivity.[5] Nevertheless, despite the innumerable studies reported so far there are still many unexplored sides of these multifaceted materials. Indeed, the property tuning of oligo- and polythiophenes has as yet mainly been focused on changes in molecular size and shape or on the grafting of various substituents to the aromatic backbone.[1] Much less attention has been devoted to the functionalization of thiophene sulfur. In thiophene, a 6 π–electrons aromatic system, sulphur has two unshared lone pair electrons, which can be employed in the formation of thiophene-S-oxides,[6] thiophene-S,S-dioxides,[7a] thiophene-sulfilimines,[7b] thiophene-sulfoximides[7bc] and thiophene- sulfonium salts.[8] Removal of thiophene sulfur lone pairs leads to the loss of thiophene aromaticity and consequent changes in frontier orbital energies.[9-10] Until now of all possible thiophene sulfur functionalizations, only sulfur dioxidation has been taken into account in thiophene based materials.[9-11] Oligo- and polythiophene-S,S-dioxides display smaller energy gaps, greater electron affinities and greater ionization energies than their non oxygenated *all*-aromatic counterparts. Very recently it has been reported that oligomers and polymers containing thiophene-S,S-dioxide groups can undergo efficient intramolecular singlet fission and are consequently candidates for the development of the next generation of photovoltaic devices based on multiple exciton-generation processes.[12] A quinque-thiophene containing one central thiophene-S,S-dioxide group has been employed for the first experimental demonstration of replica symmetry breaking in random lasers.[13] Also several biological applications of small thiophene oligomers containing thiophene-S,S-dioxide units have been reported.[5,14] A disadvantage due to the presence of thiophene-S,S-dioxide units in the molecular structure is that the materials become rapidly insoluble and intractable as the number of these

units increases, probably due to the planarity of the -SO2 group and the increased aggregation capabilities via H-bonding promoted by the presence of the two oxygens.[9d]

In this context a challenging frontier is represented by investigations on synthetic approaches to the as yet unexplored classes of oligo and polythiophene-S-oxides. These compounds should indeed be more soluble than the di-oxygenated counterparts due to the non planarity of the SO group,[6] have similar electron affinities but smaller oxidation potentials and energy gaps,[9e] hence extending the range of structure-property tunability of thiophene materials. Owing to the aromatic character of thiophene, the oxidation of thiophene sulfur requires strong oxidants such as MPBA[6] or the Rozen's reagent.[11] However, the oxidation with these reagents can hardly be be stopped at the S-oxide stage. In consequence, owing to synthetic difficulties, only spare data on oligothiophene-S-oxides[15] and no data on poly-thiophene-S-oxides have been reported so far.

In this work, we describe a synthetic platform for the facile synthesis of oligo- and polythiophene-S-oxides and -S,S-dioxides in mild condition and room T taking advantage of ultrasound assistance. We show that the cross coupling reaction of these building blocks with metalated thiophenes affords innovative regioregular oligo- and polythiophenes containing thiophene-S-oxides or mixed thiophene-S-oxide and thiophene -S,S-dioxide moieties in the desired number and position of the molecular backbone. We demonstrate that the presence of mono oxygenated thiophene units and their alternation with thiophene and thiophene-S,S-dioxide units allow for the fine modulation of properties such as frontier orbital energies, *p*- or *n*-type charge transport, photo and electroluminescence and even the biological behaviour inside live cells.

2. Results and discussion

2.1. Synthesis and characterization

The number of reagents shown in Table 1 is necessarily limited and many other examples could have been reported. Our choice was made on the grounds that thiophene S-oxides undergo more facile Diels-Alder type dimerization or other side reactions such as epoxidation of the double bond than thiophene-S,S-dioxides.[6] Rapid dimerization of the transiently formed S-oxides renders difficult the separation of many of these compounds from the reaction medium. However, studies on variously substituted thiophene rings show that stabilization of thiophene-S-oxides can be achieved by introduction of sterically hindering groups, mesomeric effects or fusion of

thiophene with phenyl as in dibenzothiophene.[6] Bromoderivatives **1-10** were prepared taking advantage of ultrasound assistance,[16] see synthetic details in SI. We have found that ultrasound assistance renders also possible the stepwise oxidation of thiophene derivatives (Table 1 and Table S2) using H_2O_2 as the oxidizing agent in CF_3COOH:DCM (1:2)[17] at roomT and employing just 1eq H_2O_2 for the S-oxide and 2eq for the -S,S-dioxide. The desired products were obtained in short reaction times and high yields while only unreacted starting compound was recovered rendering the purification step easier. Table 1 shows that with bromoderivatives **1-6** and just 1eq H_2O_2, the thiophene-S-oxide is formed in 15-30 minutes in yields varying in the range 70-99%, depending on the substrate. Times and yields are the same for the formation of the -S,S-dioxide upon addition of a second equivalent of H_2O_2. We found that also the oxidation with the classical oxidizing agent MPCBA in DCM is facilitated by the assistance of ultrasounds. In this case only the -S,S-dioxide and the starting compound are present in the reaction mixture. In our experience, in the absence of ultrasounds, a much greater amount of MPCBA would be needed; for example, for the preparation of compound **9b**, nearly 6 eq were required for overnight reaction and 52% yield.[18] Synthetic details are reported in SI. When no substituents were present in the beta positions of the thiophene ring or when alkyl chains were present (items **7-10** in Table 1) the S-oxide could not be isolated, probably due to rapid DielsAlder dimerization.[6,19] The formation of the -S,S-dioxide was instead rapid and efficient. The assistance of ultrasounds and the system H_2O_2/ CF_3COOH/ CH_2Cl_2 made the yield of **7b** (room T, 30 min, 80% isolated yield) competitive with that obtained with Rozen's reagent (room T, 1 hour, 95% yield).[20] The oxidation with MPCBA and US assistance is slower and furnishes the same yield in 90 min. From these results it is seen that the stepwise oxygenation of thiophene sulfur depends on the type of substituents on the thiophene ring. Finally, we found that for some non brominated thiophene derivatives (Table S2) the S-oxide as well as the -S,S-dioxide can be isolated in good yields upon treatment with H_2O_2 in CF_3COOH/ CH_2Cl_2 under ultrasound assistance. Afterwards both oxygenated derivates can be mono or dibrominated in the alpha positions and employed in cross coupling reactions with metalated thiophenes. The brominated S-oxides and -S,S-dioxides of Table 1 and Table S2 were stable compounds and could be purified by silicagel chromatography. Their characterization is reported in SI. IR, UV, and NMR of the S-oxides are in agreement with those reported for the thiophene-S-oxides described in the literature.[7a]

Table 1. Reagents and conditions for the ultrasound assisted synthesis of brominated thiophene-S-oxides and thiophene-S,S-dioxides.

Item	Starting compound	Product	Experimental conditions	Time (m)	Yield [a] (%)
1	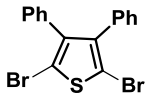	**a SO**	DCM:TFA 2:1, H_2O_2 **1 eq**	30	70
		b SO_2	DCM:TFA 2:1, H_2O_2 **2 eq**	30	80
			DCM, MPCBA **2 eq**	60	80
2	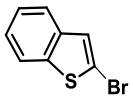	**a SO**	DCM:TFA 2:1, H_2O_2 **1 eq**	15	99
		b SO_2	DCM:TFA 2:1, H_2O_2 **2 eq**	15	99
			DCM, MPCBA **2 eq**	45	>90
3	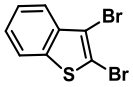	**a SO**	DCM:TFA 2:1, H_2O_2 **1 eq**	15	99
		b SO_2	DCM:TFA 2:1, H_2O_2 **2 eq**	15	99
			DCM, MPCBA **2 eq**	45	>90
4	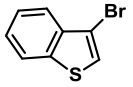	**a SO**	DCM:TFA 2:1, H_2O_2 **1 eq**	15	>90
		b SO_2	DCM:TFA 2:1, H_2O_2 **2 eq**	15	99
			DCM, MPCBA **2 eq**	45	>90
5	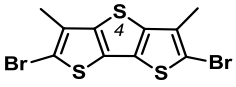	**a *4*-SO**	DCM:TFA 2:1, H_2O_2 **1 eq**	20	75
		b *4*-SO_2	DCM:TFA 2:1, H_2O_2 **2 eq**	15	90
			DCM, MPCBA **2 eq**	15	
6	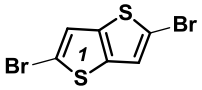	**a SO**	DCM:TFA 2:1, H_2O_2 **1 eq**	20	30
		b SO_2	DCM:TFA 2:1, H_2O_2 **2 eq**	20	90
			DCM, MPCBA **2 eq**	45	80
7	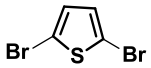	**b SO_2**	DCM:TFA 2:1, H_2O_2 **2 eq**	30	80
			DCM, MPCBA **2 eq**	90	80
8	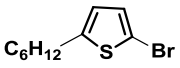	**b SO_2**	DCM:TFA 2:1, H_2O_2 **2 eq**	20	80
			DCM, MPCBA **2 eq**	20	80
9	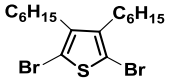	**b SO_2**	DCM:TFA 2:1, H_2O_2 **2 eq**	20	80
			DCM, MPCBA **2 eq**	20	80
10	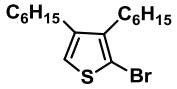	**b SO_2**	DCM:TFA 2:1, H_2O_2 **2 eq**	25	40
			DCM, MPCBA **2 eq**	60	70

a) Isolated yield.

Oligo- and poly-thiophenes having thiophene-S-oxide and/or thiophene-S,S-dioxide groups in precise position and number in the molecular backbone could easily be prepared by reacting compounds **1a-6a** and/or **1b-6b** and **7-10** with metalated thiophenes via palladium catalyzed cross-coupling Stille or Suzuki reactions[21] to obtain the formation of the desired products in high yields. A few examples of the innumerable structures that can be prepared on the basis of the simple chemical strategy described above are given in Schemes **1-4**. Scheme 1 shows the synthetic pattern to prepare oligomers and polymers starting from dibromo derivatives **1a** and **1b**. The polymers (**1a1,1b1**) are made of alternating 3,4-diphenyl-thiophene and 3,4-diphenyl-thiophene-S-oxide or -S,S-dioxide units. The oligomers are trimers (**1a3,1b3**) or pentamers (**1a2,1b2**) with one central thiophene-S-oxide or -S,S-dioxide and hexamers bearing two thiophene-S-oxide or -S,S-dioxide groups (**1a5** and **1b5**, respectively) or one thiophene-S-oxide and one thiophene-S,S-dioxide group (**1ab**).

Scheme 1. Preparation of oligomers and polymers from 2,5-dibromo-3,4-diphenyl-thiophene-1-oxide **1a** and -1,1-dioxide **1b**.

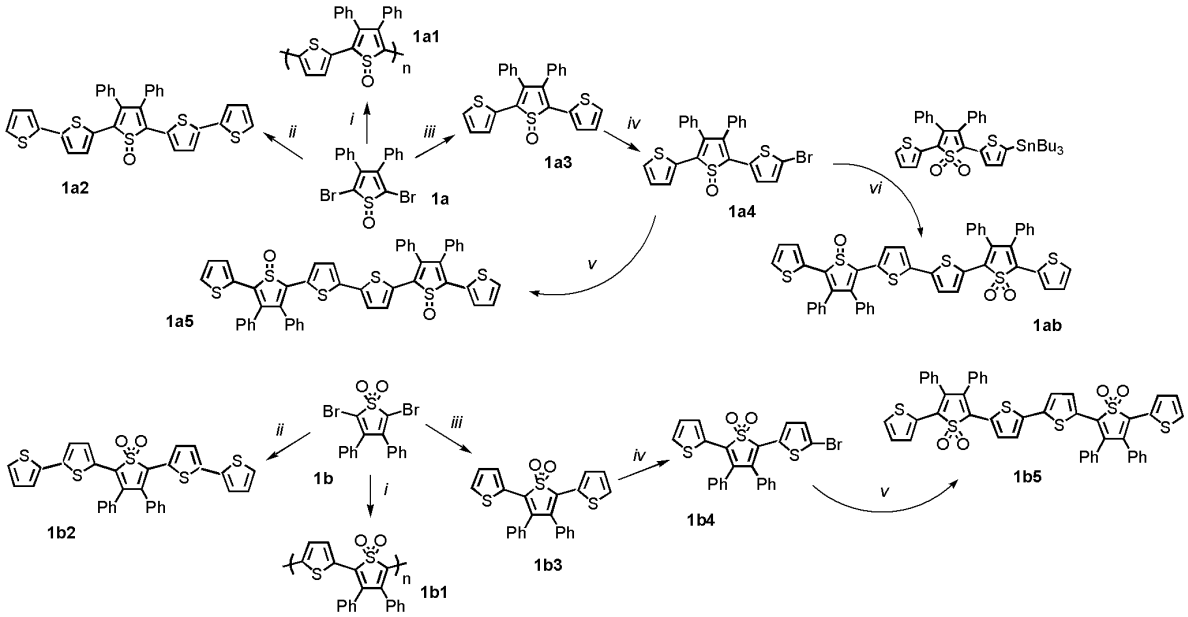

i) 2,5-bis(tributylstannyl)thiophene, ii) 2-tributylstannyl-2:2'.bithiophene, iii) 2-(tributylstannyl)thiophene, Pd $(PPh_3)_4$, toluene, reflux overnight; iv) N-bromosuccinimide , CH_2Cl_2 : CH_3COOH, US; v) Bis (pinacolato)diboron, $PdCl_2dppf$, $NaHCO_3$, THF:H_2O 2:1, MW, 80°C; vi) **1a4a**, Pd $(PPh_3)_4$, toluene, reflux overnight. US=ultrasound assistance, MW=microwave assistance. Details in SI.

Scheme 2 illustrates the preparation of V-shaped[22] oligomers obtained from **3a** and **3b**, while Scheme 3 describes the pattern to obtain the polymer, **5a2**, with alternating mono- and dioxygenated thiophene units.

Scheme 2. Preparation of V-shaped oligomers from 2,3-dibromo-benzo[b]thiophene-S-oxide **3a** and -S,S-dioxide **3b**.

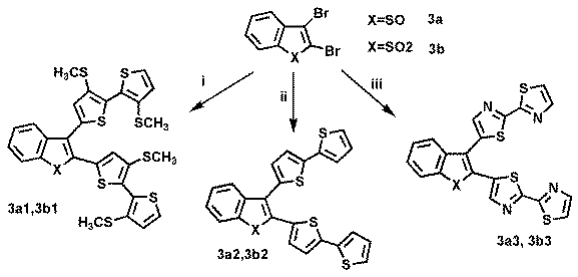

i) 5-tributylstannyl-3,3'-bis(methylthio)-2,2'-bithiophene , ii) 2-tributylstannyl-2,2'-bithiophene, iii) 5-tributylstannyl-2,2'-bithiazole, Pd $(PPh_3)_4$, toluene, reflux overnight. Details in SI.

Scheme 3. Preparation of oligomers from 2,6-dibromo-3,5-dimethyl-dithieno[3,2-b:2′,3′-d]thiophene-4-oxide **5a** and -4,4-dioxide **5b**.

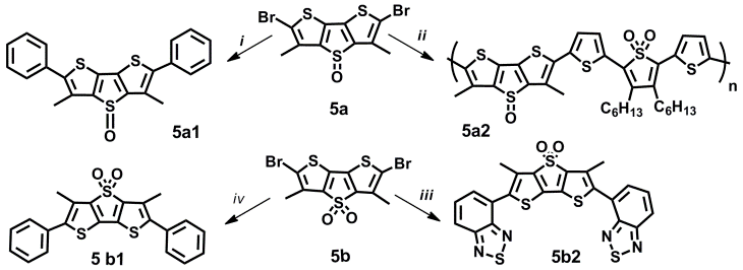

i) **5a** (1 mmol), phenylboronic acid pinacol ester (3 mmol), $PdCl_2$dppf (0.05 mmol) and $NaHCO_3$ (2 mmol) in THF/water 2:1 (3 mL), MW, 15'; ii) **5a**, 3',4'-dihexyl-5,5"-bis(tributylstannyl) - [2,2':5',2"-terthiophene]1',1'-dioxide iii) **5b** (1 mmol, 4-(4,4,5,5-tetramethyl-1,3,2-dioxaboralan-2-yl)-2,1,3-benzothiadiazole (3 mmol), $PdCl_2$dppf , $NaHCO_3$, THF/H2O 2:1, MW; iv) **5b**, phenylboronic acid pinacol ester, $PdCl_2$dppf, $NaHCO_3$, THF/H2O 2:1, MW. For 5b1 see reference 15c. Details in SI.

Scheme 4 describes the preparation of a quinquethiophene having one (**9b1**), two (**10b3**) and three (**9b4**) thiophene-S,S-dioxide groups in the backbone.

Scheme 4. Preparation of pentamers from 2,5-dibromo-3,4-dihexyl-thiophene-1,1-dioxide **9b** and 2-bromo-3,4-dihexyl-thiophene-1,1-dioxide **10b**.

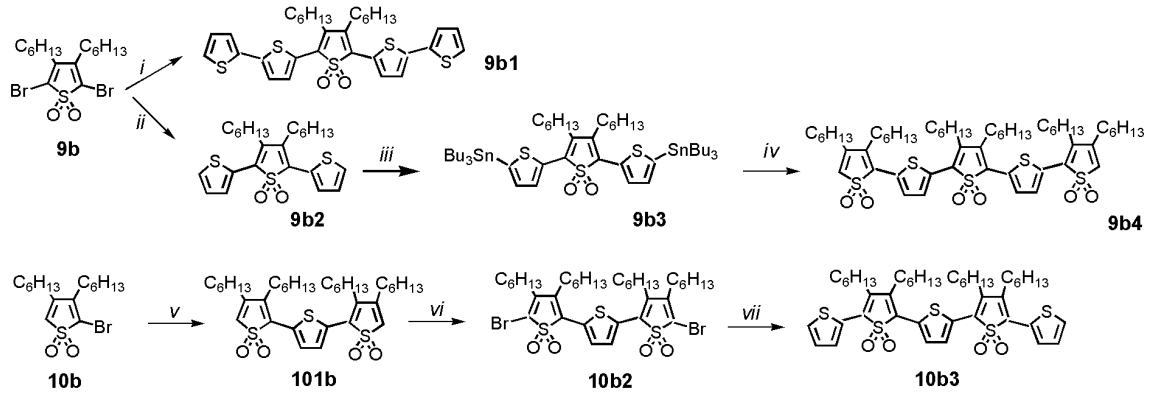

i) 2-(tributylstannyl)-2,2'-bithiophene, ii) 2-(tributylstannyl)- thiophene, Pd $(PPh_3)_4$, toluene, reflux overnight; iii) THF, BuLi, Bu_3SnCl; iv) **9b**, v) 2,5-bis(tributyl)- thiophene, Pd $(PPh_3)_4$, toluene, reflux overnight; vi) N-bromosuccinimide , CH_2Cl_2 : CH_3COOH, US; vii) 2-tributylstannyl)-thiophene, Pd $(PPh_3)_4$, toluene, reflux overnight. Details in SI.

As predicted, the oligomers containing only thiophene-S-oxide units were much more soluble in common organic solvents than those containing alternating thiophene-S-oxides and thiophene-S,S-dioxides and even more soluble than those containing only thiophene-S,S-dioxides units. Polymers **1a1** and **1b1** were weakly soluble in THF, while **5a2** displayed significant solubility attributable to the presence of long side-chains. The characteristics of polymers **1a1**,**1b1** and **5a2** are reported in Table S1.

***2.1.1. Single crystal X-ray structure of hexamer* 1a5**. There are only spare data on single crystal X-ray structure and conformation of thiophene-S-oxides.[9a,23] We have been able to obtain single crystals for hexamer **1a5** having a backbone containing two thiophene-S-oxide units. The X-ray diffraction molecular structure and packing of **1a5** are reported in Figure 1. The compound has a crystallographic inversion centre in the middle of the C-C bond connecting the inner thienyl rings. The orientation of the sulfur atoms in the adjacent rings is transoid. The central bithiophene unit is planar and is connected in the 2-positions to the thiophene-1-oxide rings bearing two phenyl groups in 3 and 4 and a thienyl ring in 5. The ring containing the oxidized sulfur atom loses its aromatic character and shows a diene structure with C5-C6, C6-C7 and C7-C8 bond distances of 1.354(7), 1.474(7) and 1.380(7) Å, respectively. In agreement with the already reported X-ray data,[9a,23] the oxidized sulfur exhibits a pyramidal geometry and lies 0.186 Å out of the C5-C6-C7-C8 least-square plane. In addition, the S2-C bonds (S2-C5

1.816(5) and S2- C8 1.794(6) Å) are longer than the S-C distances in the other thiophene rings that fall in the range 1.683 -1.749(5) Å. The C5-C6-C7-C8 mean plane makes dihedral angles of 20.1(3) and 8.7(3)° with the outer and inner thienyl rings, respectively. The deviation from planarity of the thiophene-S-oxide sulfur is small, indicating the possibility that some π-delocalization may still occur.

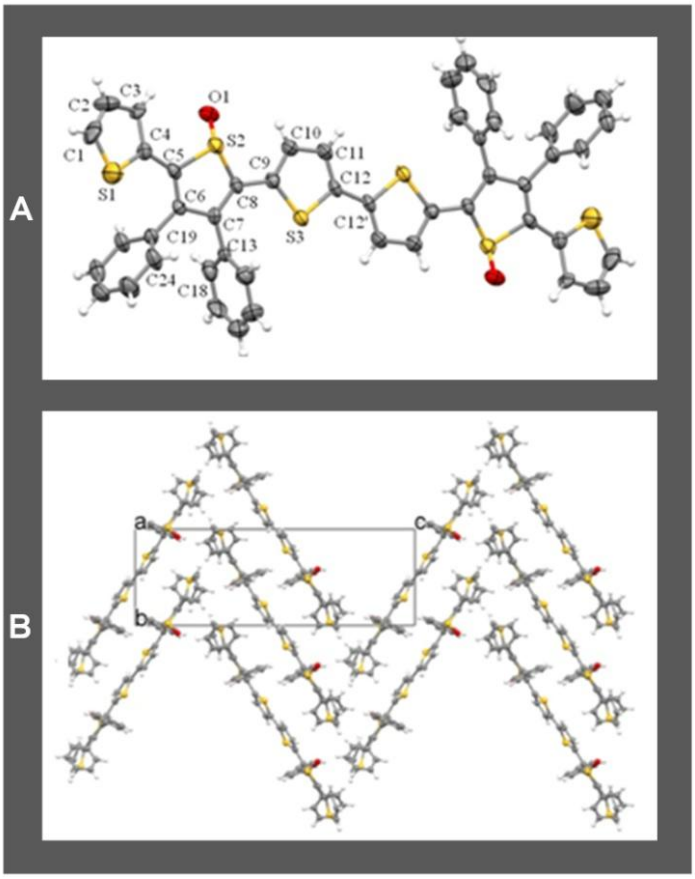

Figure 1. Figure 1. Crystal structure of hexamer **1a5** containing two thiophene-S-oxide moieties. A) Molecular conformation. The labeled atoms are related to the unlabelled ones by the symmetry operation –x+1, -y, -z+1. B) View down the *a* axis of the crystal packing.

In the crystal the molecules adopt a pseudo-herringbone mode (Figure 1 B). The molecules pack in a parallel slipped arrangement but without π-π stacking (distance between the molecular plane 4.45 Å). The intermolecular interactions between the different stacks are mainly C-H…π interactions (H20-centroid(C19-C24) 3.43 Å. It is worth noticing that the crystal conformation of **1a5** closely resembles the recently reported substituted hexamer having butyl groups in place of

the phenyl rings, one methyl group in the outer thiophene ring and two thiophene -S,S-dioxides instead of two thiophene-S-oxide moieties.[24]

2.2. Electrochemical characterization. Cyclic Voltammetry was used to measure the redox potentials of the newly synthesized oligomers and polymers and to estimate the HOMO-LUMO electrochemical energy gaps. Table 2 reports the oxidation and reduction potentials and the corresponding energy gaps as well as HOMO and LUMO energies calculated according to known modalities.[25] Representative CV scans are shown in Figure 1-2. All plots are reported in SI (Figures S17-S22).

It is seen that the presence of thiophene S-oxides results in lower oxidation potentials and lower (more negative) reduction potentials than the presence of thiophene-S,S-dioxides in the corresponding molecular structure. Compare, for example, polymers **1a** and **1b** or pentamer **1a5** and **1b5**. Generally, the shift of the oxidation potential is more significant than that of the reduction one hence the electrochemical energy gaps of oligo/polythiophene-S-oxides are smaller than those of the corresponding oligo/polythiophene- S,S-dioxides. Polymers **1a1**, **1b1** and **5a2** whose CV plots are shown in Figure 1, having the HOMO-LUMO energy gap < 2 V, are all Low Band Gap polymers.[26] The optical energy gaps, estimated by the onset point of the absorption bands in solution (Figure 1) are in agreement with the electrochemical energy gaps. Polymer **1a1** has one of the lowest electrochemical gaps of polythiophenes described to date, 1.25 V. Remarkably, both polymers **1a1** and **1b1** display reduction potentials similar to those of PCBM,[27] indicating significant electron affinities. The reduction potential of the mixed polymer **5a2**, with a different molecular structure, is sizeably more negative than that of the other two polymers while the energy gap is much higher (1.92 V). Of the series of hexamers bearing two oxidized thiophenes, namerly compounds **1a5** (two S-oxides), **1b5** (two -S,S-dioxides) and **1ab** (one S-oxide and one -S,S-dioxide) - see the CV plots in Figure S17 - the former displays the lowest oxidation potential (1.08V), the second the highest (1.42V) while the third is intermediate between the two (1.14V). The comparison of the redox potentials of pentamers **9b1, 10b3** and **9b4** (see CV plots in Figure S18) shows that passing from one thiophene-S,S-dioxide unit to two and three in the same molecular skeleton leads to a progressive increase in ionization potential paralleled by a progressive increase in reduction potential. Thus, the advantage of increasing the electron affinity of the system is paid by the increase in ionization energy.

Table 2. Redox potentials of oligo/polythiophene-S-oxides, -S,S-dioxides and mixed -S-oxides/-S,S-dioxides

	$E_{ox(onset)}$ *V vs SCE*	$E_{red(onset)}$ *V vs SCE*	E_g *eV*	*HOMO eV*	*LUMO eV*		$E_{ox(onset)}$ *V vs SCE*	$E_{red(onset)}$ *V vs SCE*	E_g *eV*	*HOMO eV*	*LUMO eV*
1a1	0.69[a]	- 0.56[a]	1.25	5.37	4.12	**3a1**	1.04[c]	-1.31[c]	2.35	5.72	3.37
1b1	0.98[c]	- 0.49[a]	1.37	5.66	4.19	**3b1**	1.09[b]	-1.25[c]	2.34	5.77	3.43
5a2	0.95[a]	- 0.97[c]	1.92	5.63	3.71	**3a2**	1.20[c]	-1.28[c]	2.48	5.88	3.40
						3b2	1.35[a,d]	-1.19[a,d]	2.54	6.03	3.49
1a3	1.29[c]	-1.25[b]	2.54	5.97	3.43	**3a3**	>1.6	-1.08[c]	>2.68	> 6.28	3.60
1b3	1.47[c]	-1.11[a]	2.58	6.15	3.57	**3b3**	>1.6	-0.9[c]	>2.51	> 6.28	3.77
1a5	1.08[b]	-1.19[b]	2.27	5.76	3.49						
1b5	1.42[c]	-0.92[b]	2.34	6.1	3.76	**5a1**	1.23[c]	-1.53[b]	2.76	5.91	3.15
1ab	1.14[c]	-1.04[c]	2.18	5.82	3.64	**5b1**	1.47[c]	-1.48[c]	2.95	6.15	3.20
1a2	1.04[b]	-1.18[c]	2.22	5.72	3.50	**5b2**	1.46[b]	-1.25[c]	2.71	6.14	3.43
1b2	1.16[c]	-1.03[c]	2.19	5.84	3.65						
						9b1	1.22[a]	-1.20[a]	2.42	5.9	3.48
						10b3	1.38[b]	-1.00[a] -1.10[c]	2.38	6.06	3.68
						9b4	1.46[b]	-0.94[c]	2.40	6.14	3.74

[a]Reversible. [b]Irreversible. [c] Quasi-reversible. [d]Reference 22.

The three dithienothiophene derivatives, **5a1**, **5b1** and **5b2** – see CV plots in Figure S19 – display quasi-reversible oxidation waves. On the contrary, only **5b1** with two terminal benzothiadiazole units, displays a reversible reduction wave, the other two being irreversible. Note that the oxidation potential of **5b2** is very close to that of **5b1** having two phenyl groups, suggesting that the HOMO of the former is mainly concentrated on the dithienothiophene-S,S-dioxide unit.

2.3. Optical properties. Absorption and emission wavelenghs and molar absorption coefficients of all oligomers and the absorption wavelength of all poymers are reported in Table S3. The corresponding spectra are shown in Figure 1 and Figures S23-S30. To time the photophysical properties of oxygenated thiophene derivatives have been poorly investigated. Very recently, Busby, E. et al. have reported that the photodynamics of compounds containing thiophene-S,S-oxide moieties is profoundly different from that of the non-oxygenated counterparts,[28] owing to the formation of fast singlet deactivation pathways which reduce the excited state lifetime by several orders of magnitude depending on the number and sequence of oxygenated thiophene

units present in the molecular structure. Probably due to analogous reasons, none of polymers **1a1**, **1b1** and **5a2** displays light emission in the visible or NIR range upon irradiation at the maximum absorption wavelength. The oligomers having only one single inner thiophene-S,S-dioxide or thiophene-S-oxide moiety - whether in linear trimers (**1a3**, **1b3**, Figure S28) and pentamers (**1a2**, **1b2**, Figure S24) or in V-shaped systems (**3a1-3**, 3**b1-3**, Figure S25) or in dithienothiophene derivatives (**5a1**, **5b1**, **5b2**, Figure S27) - display hotoluminescence in the visible region. However, on increasing the number of oxygenated units present in the molecular backbone, the intensity of the photoluminescence signal progressively decreases. This effect is nicely illustrated by the sequence of pentamers **9b1**, **10b3** and **9b4** having one, two and three thiophene-S,S-dioxide moieties, respectively, in the backbone. Figure S23 shows that the photoluminescence progressively vanishes as the number of S,S-dioxide moieties increases.

Table 3. Maximum emission wavelengths, decay times τ1, τ2, τ3 and photoluminescence quantum yields of 3a1 and 3b1.

	λ (nm)	**τ1 (ns)**	**τ2 (ns)**	**τ3 ns**	**PLQY %**
3b1 1.0^{-5} M in DCM	650	0.8		5.3	n.d.
3b1 0.1% in PMMA	600	1.1		5.6	19%
3b1 100 %	650	0.6	2.0	4.4	0.7%
3a1 1.0^{-5} M in DCM	650	0.8		5.6	n.d.
3a1 0.1% in PMMA	650	1.0		5.6	11 %
3a1 100 %	650	0.7	2.6	7.8	0.4%

A similar effect is observed for the hexamers having two thiophene-S-oxide groups (**1a5**), two thiophene-S,S-dioxide groups (**1b5**) and one thiophene-S-oxide and one thiophene-S,S-dioxide group (**1ab**), which display the same absorption spectra and extremely weak photoluminescence spectra in solution (Figure S24). Of the three hexamers only the former one displays a sizeable photoluminescence signal in cast film (Figure S26). Although we are aware of the fact that only deeper photophysical studies - far beyond the objective of the present study - would allow to unambiguously shed light on the photophysical properties of oxygenated thiophene derivatives, to give an insight into the properties of the newly synthesized compounds Figure S29 compares the spectra of **3a1** and **3b1** in $1.0x10^{-5}$ M solution in DCM, in thin film 0.1wt% in PMMA and in neat film (100%). The UV-Vis spectra show that passing from isolated monomers dispersed into the PMMA inert matrix to the neat film there is a considerable red shift indicating the

formation of aggregate absorbing states (dimers).[29,30] The isolated monomer absorption profile for both oligomers finely match that obtained in solution. The photoluminescence spectra show that for both compounds the spectral profiles change considerably passing from 0.1% in PMMA to the pure dye for which a marked red shift is again observed. The red shift of about 60 nm in both oligomers can be ascribed to the interaction of adjacent molecules leading to the formation of dimer emitting states. According to the data reported in Table 3 the highest photoluminescence quantum yields (PLQY) are those of the samples 0.1 % in PMMA (ΦPL ~ 0.1, 0.2) and the lowest those of the pure samples (ΦPL = 0.04, 0.07), possibly due to quenching activities of the excited states by molecular oxygen and/or self-quenching phenomena.

2.4. Thin film devices. Here we report experimental evidence that thiophene-S-oxides are charge transporting and electroluminescent materials and that - in contrast to non-oxygenated oligo/polythiophenes and to the corresponding –S,S-dioxides (*p*-type and *n*-type semiconductors, respectively) they are ambipolar semiconductors.

2.4.1 Field-effect transistors with polymers 1a1, 1b1 and 5a2. The polymers were tested as active materials in staggered top-gate FETs operating both in *p*- and *n*-accumulation regimes. A staggered architecture was adopted since it typically suffers less from charge injection limitations at the contacts,[31] and a top-gate configuration with alow-k polymer dielectric, in this case PMMA, offers a dielectric/polymer interface which is more ideal for charge transport.[32] The measured transfer curves (Figure 2B) for the fabricated devices highlight a capability of all three materials for electron transport, while only **1a1** and **5a2** - having thiophene-S-oxide units - can appreciably conduct holes. It is to stress how the ambipolarity feature of the latter two materials is fairly balanced with respect to the opposite charged species. The extracted mobility values for the materials are summarized in Figure 2Bd. To date FET charge mobilities of polymers bearing thiophene-S,S-dioxides moieties into the aromatic backbone have been assessed only in two cases. The first case concerns a polythiophene with varying ratios of alkylated thiophene to thiophene-S,S-dioxide units in the backbone.[33a] According to that study I-V measurements showed that the polymers never exhibited clear field-effect behavior in either hole or electron accumulation regimes. Moreover, the authors report that the SO2 functionality was labile on heating and increasing above 50% the number of oxygenated thiophene units present in the backbone resulted in significant degradation negatively impacting on charge-transport properties.

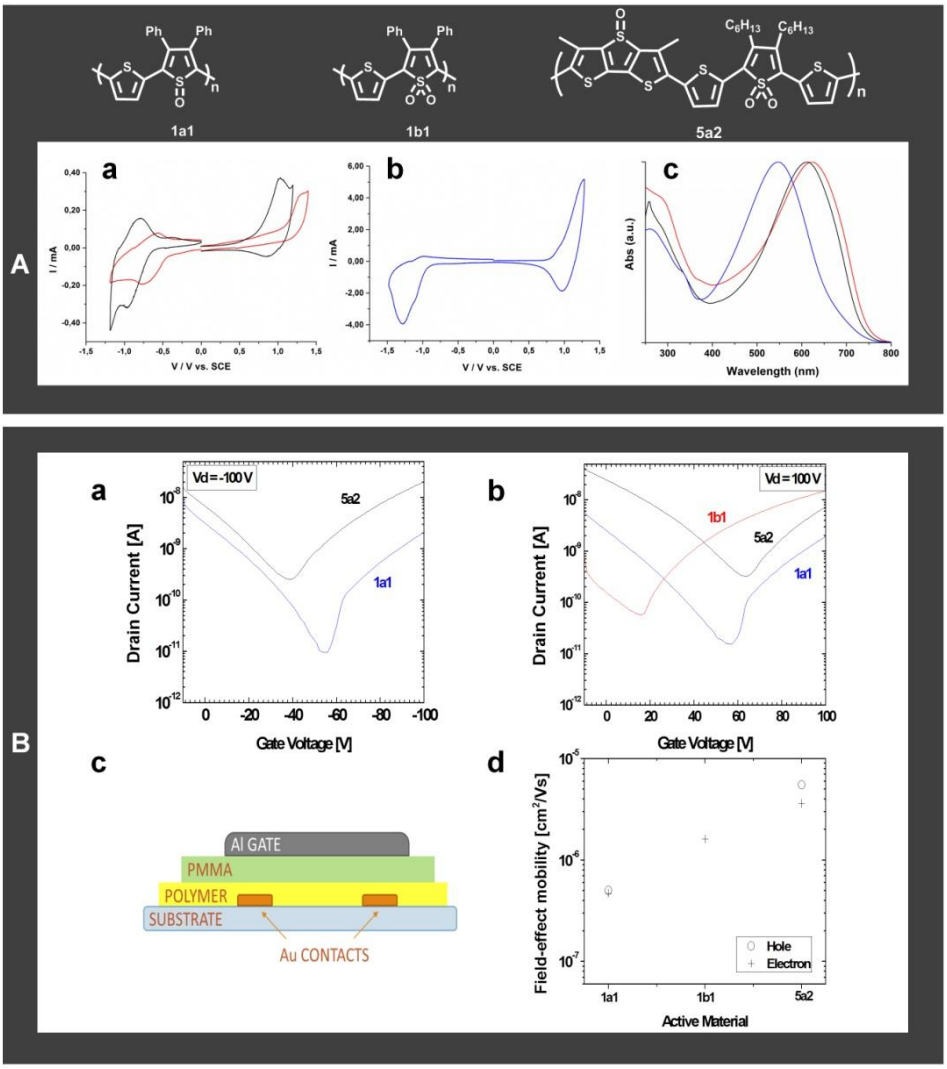

Figure 2. A) Cyclic voltammetries of polymers 1a1, **1b1**, **5a2** (a,b) and absorption spectra in DCM (c). B) Transfer curves for the fabricated FETs in (a) hole accumulation regime (V_{drain} = -100 V) and (b) electron accumulation regime (V_{drain} = 100 V); the FETs stack (c); (d) the extracted Field-Effect charge mobilities for the polymers. Geometrical dimensions for the FETs channel are L = 20 µm for polymers **5a2** and 1b1, L = 10 µm for polymer **1a1** and W = 10 mm in all cases.

In particular they report that an incorporation of oxygenated thiophene higher than 20% led to complete failure of the FETs after a 110 °C thermal annealing. By contrast, the FET devices reported here, realized using active materials featuring 30 to 50% incorporation, showed proper field-effect behavior even after a thermal annealing at 150 °C. The second case concerns two polymers alternating acenaphtho [1,2-c]thiophene-S,S-dioxide units and thieno-thiophene or

benzo [1,2-b:4,5-b']dithiophene units.[33b] The polymers displayed *p*-type charge mobility on the order of $10^{-3} – 10^{-4}$ $Vcm^{-1}s^{-1}$.

It is well known that FET charge mobilities can be enhanced by optimizing device fabrication and film morphology[31,32,34] or appropriate surface treatment.[35] The optimization of film morphology requires a good knowledge of the self-assembly properties of oligomers and polymers bearing thiophene oxidized moieties in the backbone. Although some data are available on single crystal X-ray structure of oligothiophene-S,S-dioxides[36] and powder X-ray studies of polythiophene-S,S-dioxides outlining the importance of H-bonding on molecular packing,[37] no detailed investigations have been carried out so far on the self-assembly pathways in thin films of oligomers and polymers containing thiophene oxigenated units. It is reasonable to expect that these studies will result in the preparation of thin films with optimized morphology and consequently higher charge mobility values than those reported in Figure 1B. However, independently of the FET charge mobility values, our data unambiguously indicate that charge carrier types in thiophene materials can be modulated via mono- or di-oxygenation of thiophene sulfur. Concerning the compounds containing thiophene-S-oxide units in the backbone, we suggest that their ambipolar charge conduction properties related to lower oxidation potentials compared to the corresponding compounds having thiophene-S,S-dioxide units.

2.4.2 Light emitting devices with oligomers 3a1 and 3b1. Further evidence that oligothiophene-S-oxides have ambipolar charge transport properties while the corresponding –S,S-dioxides are *n*-type charge carriers comes from comparison of electroluminescent devices with V-shaped oligomers **3a1** and **3b1**. It is known that V-shaped thiophene-S,S-dioxides are active materials in electroluminescent devices,[22] that they form non centro-symmetric thin films and one member of the series displays second order susceptibility $\chi^{(2)}$ values as high as the reference LiNbO3 single crystal, without poling processing.[38] No data are available for the corresponding S-oxides.

Light emitting diodes were fabricated using either the neat films of both **3a1** and **3b1** or films where the compounds were dispersed in 15% concentration (chosen following optimized photoluminescence quantum yield yield measurements) within two different host matrices: BCPO, namely ambipolar 9,9′-(4,4′-(Phenylphosphoryl) bis-(4,1-phenylene))bis(9H-carbazole) and TPBI, namely electron transporting 1,3,5-tris-(N-phenylbenzimidazole-2-yl)-benzene. Both compounds were electroluminescent systems as shown in Figure 3, Figure S31 and Figure S32.

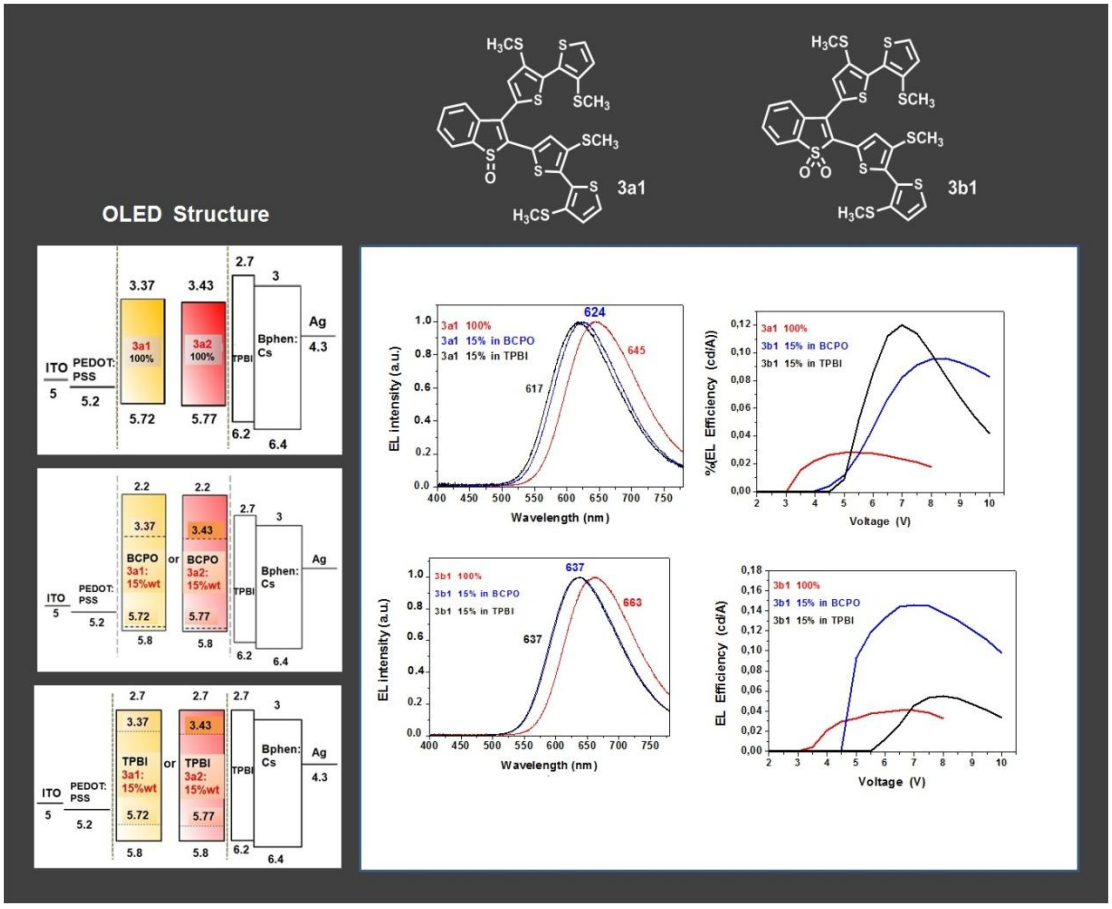

Figure 3. Structure of electroluminescent devices, electroluminescence intensity and efficiency of V-shaped oligomers **3a1** and **3b1** in thin films, 15% in BCPO, namely bipolar 9,9′-(4,4′-(Phenylphosphoryl)bis-(4,1-phenylene))bis(9H-carbazole) and 15% in TPBI, namely electron transporting 1,3,5-tris-(N-phenylbenzimidazole-2-yl)-benzene.

Figure 3 shows that the electroluminescent spectra are in accordance with the photophysical characterization displaying emission peaks around 620 nm (**3a1**) and 635 nm (**3b1**) for the host-guest system light emitting diodes (LEDs) and around 645 nm and 660 nm, respectively, for LEDs with neat films. Due to self-quenching phenomena in the neat films, high current density values are measured, demonstrating an inefficient exciton radiative recombination within the emitting layers, which leads to low luminance and low current efficiencies. In the case of host-guest systems better results were obtained in terms of luminance and current efficiencies. Figure 3 shows that the S-oxide **3a1** exhibits close values of electroluminescence efficiency in both

matrices with the highest one being obtained for the film dispersed within the ambipolar BCPO matrix. By contrast, there is a much greater difference in the electroluminescence efficiency of **3b1** dispersed into the two different matrices, the highest value being attained when the compound is dispersed within the electron transporting TPBI matrix. Since the electro-optical characteristics of the devices depend on the intrinsic transport properties of the active materials[39] it can be argued that the S-oxide **3a1** has ambipolar charge transport properties whereas **3a2** has a predominant electron transporting behaviour.

3.6. Oligomers 5a1, 5b1 and 5b2 inside live cells. The presence of thiophene-S,S-dioxide moieties into the molecular backbone not only changes the frontier orbital energies but also affects the aggregation properties through the formation of H-bondings involving the oxygen atoms. We have already reported that the green fluorescent dithienothiophene -S,S-dioxide **5b1** is able to spontaneously cross the membrane of live mouse and bone-marrow human tumour fibroblasts.[14a,b,d] In the perinuclear region **5b1** is recognized by the hydroxy proline component of protocollagen polypeptide chains through the formation of hydrogen bondings between the O-H group of hydroxyproline and the oxygen atom of the O=S=O group. As a consequence, the formation of co-assembled fluorescent and conductive type-I collagen-**5b1** microfibers is observed inside the cells. Having now the possibility to prepare in fair amount and free of contaminants the corresponding S-oxide, **5a1**, we could repeatedly and reproducibly test its behaviour inside live cells in the same conditions. The results are reported in Figure 4A and Figure 4B comparing the behavior of **5a1** and **5b1**. Figure 4A shows the formation of fluorescent microfibers after 6 hours (a) and 120 h (b) upon spontaneous uptake of **5b1** by live human fibroblasts. The diffusion of **5b1** inside the cells is rather uniform as the cytoplasm appears entirely stained, while the compound does not enter the nucleus of the cells which remains dark. Figure 4A(c-e) shows that most microfibers display helical supramolecular organization, as indicated by 3D Laser Scanning Confocal Microscopy (LSCM) reconstruction. The fluorescent microfibers are mainly made of type-I collagen co-assembled with **5b1**, as demonstrated by SDS-PAGE and immunoblotting analysis.[14a,b,d] Similar to **5b1**, sulfoxide **5a1** - also green fluorescent - is also able to be spontaneously internalized by live NIH 3T3 mouse fibroblast cells without altering their viability and proliferation ability. Figure 4 reports the MTT cytotoxicity tests[40] on NIH 3T3 cells treated with **5a1** and a few other S-oxides and -S,S-dioxides. The corresponding cytotoxicity test for **5b1** is reported in reference 14d.

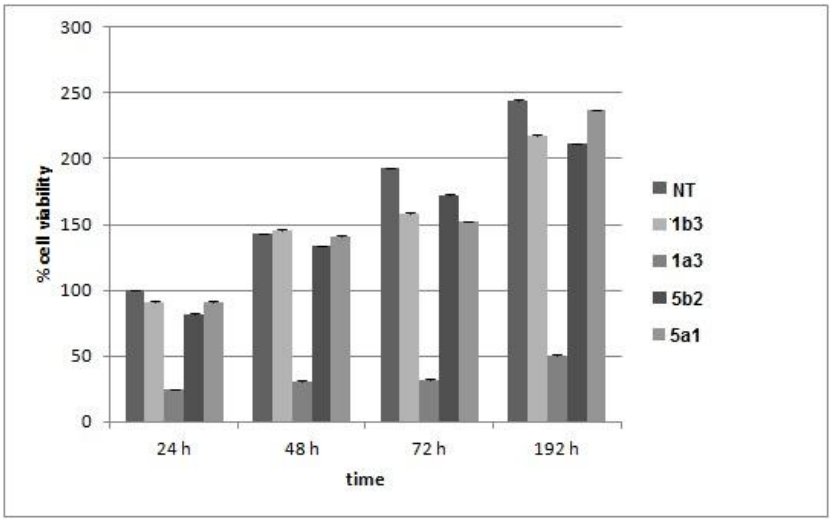

Figure 4. MTT cytotoxicity tests on NIH 3T3 cells treated with **1b3**, **1a3**, **5b1** and **5a1** compared to untreated cells (NT). Representative measurements of three distinct sets of data and no significant difference between values at different time points is observed at $P < 0.05$ with t-Student test. See reference 14d for **5b1**.

Contrary to the -S,S-dioxide **5b1**, the S-oxide **5a1** once internalized by the the cells is not recognized by any intracellular component and is physiologically and progressively eliminated. Figure 5B shows that after 24h from spontaneous uptake by the fibroblasts, **5a1** accumulates in the perinuclear region forming bright green fluorescent spots. However, there is no sign of formation of fluorescent fibers and after 168h (7 days) only a few fluorescent aggregates of **5a1** are still present inside the cells.

To account for the different behaviour of the mono-oxygenated **5a1** with respect to the di-oxygenated **5b1** inside the cells we performed a theoretical study using the density functional theory at the BLOC-D3/def2-TZVPP level.[41] To elucidate the nature of the non-covalent interaction between the S-oxide and collagen, and especially the role of the hydrogen bonding, an analysis of the reduced gradient as a function of the electron density (ρ) times the second eigenvalue of the electron-density Hessian (λ_2) was performed in the collagen-5a1 (5b1)· · ·Collagen [C-5a1 (5b1)…C] bonding region. This is the so called NCI indicator, which is able to characterize different kinds of non-covalent bonds.[42]

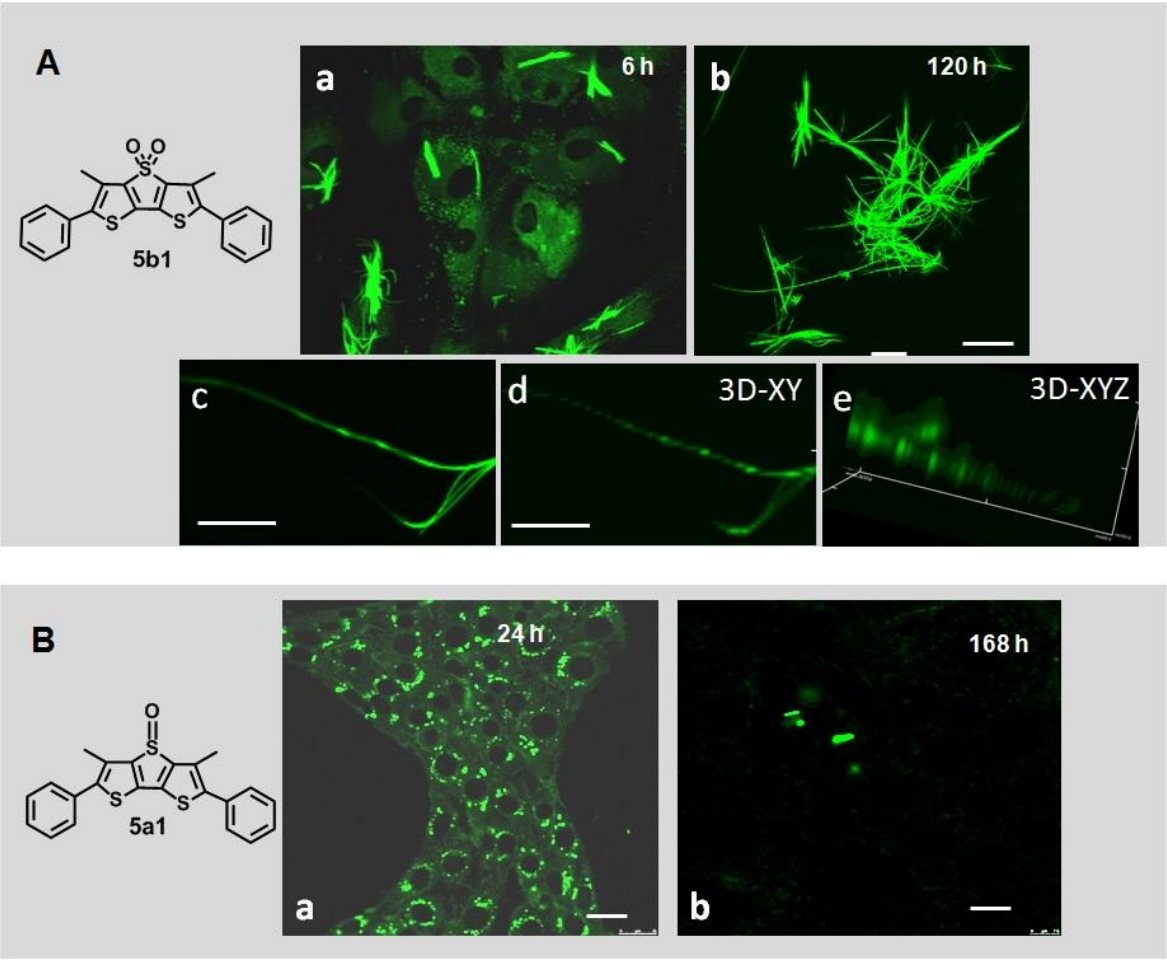

Figure 5. LSCM images of live fibroblasts upon spontaneous uptake of 5b1 and 5a1. A) View (a,b) of the cell culture after 6 and 120 hours from uptake of 5b1 by human fibroblasts showing the formation of green fluorescent microfibers on the surface of the cells (scale bars: 25 μm), a detail of the microfibers structure (c) and the corresponding 3D spatial reconstruction (d,e) displaying the helical morphology of the microfibers (scale bars: 50 μm (c); 25 μm (d,e)). B) LSCM images of live N3 HT3 fibroblasts 24h (a) and 168h (b) from spontaneous uptake of 5a1 showing that in this case there is no formation of fluorescent microfibers (scale bars: 75 μm).

Since the fluorescent microfibers generated by the cells upon uptake of **5b1** are mainly made of type-1 collagen, the theoretical investigation considered a model system consisting of one molecule (either **5b1** or **5a1**) sandwiched between two collagen strands simulated by a sequence of three tripeptide Gly-Pro-HyPro (Figure 6A). A similar model for collagen but with only a single tripeptide chain was also used in reference 14d.

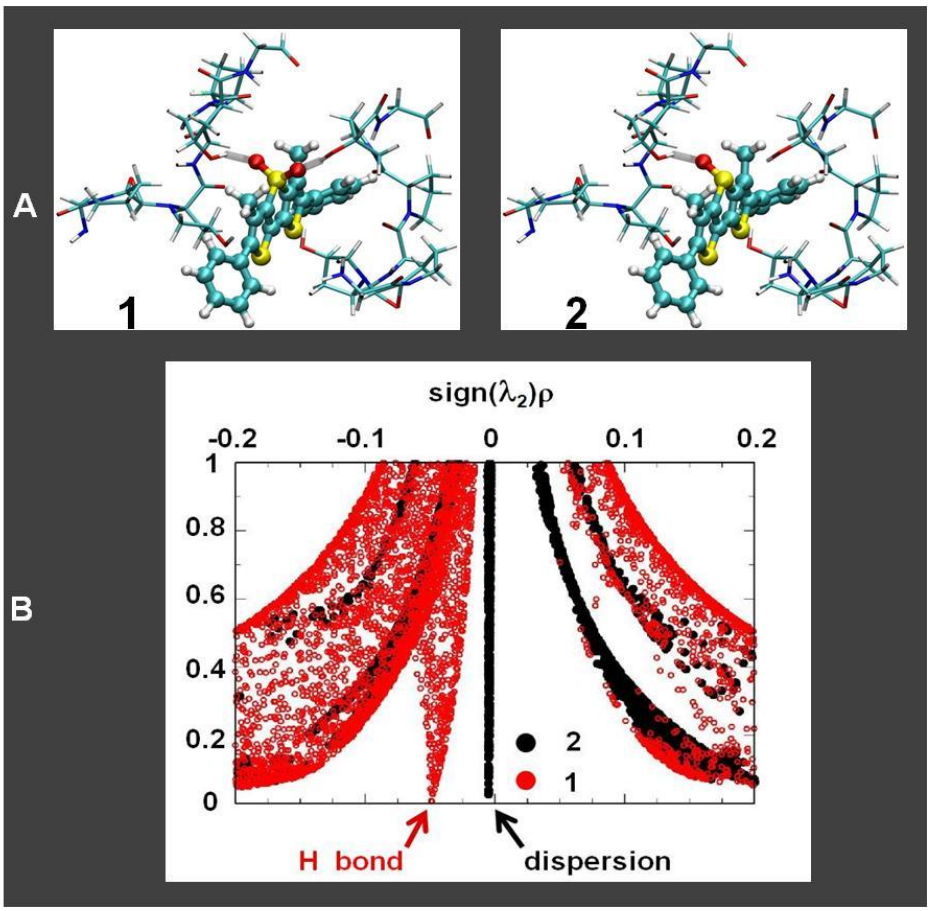

Figure 5. A) Model systems considered for DFT calculations with **5b1 (1)** and **5a1 (2)** interacting with two collagen strands built up of three Gly-Pro-HyPro tripeptide chains. B) NCI indicator analysis of the bonding region between the Collagen-Fluorophore and the additional collagene strand in cases 1 and 2. In the x-axis label ρ denotes the electron density and λ_2 the second eigenvalue of the electron-density Hessian.

The results of this analysis, reported in Figure 5, unambiguously show the importance of oxygen to promote a H-bonding between the oxidized compounds and the collagen strand. In fact, in the case of -S,S-dioxide **5b1** (case 1) a clear hydrogen bond nature is observed due to the interaction of the oxygen atoms with the hydrogen atoms of the HyPro rings in front of it. By contrast, when the corresponding S-oxide **5a1** is considered (case 2), where no oxygen

atom is present to mediate the interaction between C-F and the second collagen strand, no signature of hydrogen bonding was found in the relevant bonding region and the interaction between **5a1** and the collagen strand is only due to dispersion contributions. These results not only provide a key to understand why **5a1** does not lead to the physiological formation of fluorescent microfibers, but also confirm our previous interpretation according to which the collagen-**5b1** co-assembly inside live fibroblasts is mainly due to the hydrogen bonding capabilities of the sulfone groups.[14d]

We can anticipate that we have tested several other thiophene-S,S-dioxides and the corresponding S-oxides for their behaviour inside live cells. We have found that the former were not toxic to the cells (as shown in Figure 4 for **1b3** and **5b2**) and always formed fluorescent microfibers inside the cells, the composition of which varied with the molecular structure and is currently under study. On the contrary, the corresponding S-oxides never led to the formation of fluorescent microfibers inside live cells and some of them were even toxic to the cells (as shown in Figure 4 for **1a3**).

3. Conclusion

The straightforward and low cost chemical strategy outlined in this work opens a wide range of opportunities for the development of innovative thiophene materials with tailored properties and function. It relies on the easy synthesis of mono-oxygenated thiophene units, namely thiophene-S-oxides, very difficult to access with previously developed synthetic methodologies for thiophene oxygenation. Mono-oxygenated, di-oxygenated and non-oxygenated thiophene units can be viewed as Lego bricks which can be mixed at will to create innumerable new molecular structures to add to the already vast land of thiophene materials with little synthetic effort. The introduction of thiophene-S-oxides into the conjugated backbone of polythiophenes has several consequences, in particular a marked increase in electron affinity which, in contrast with the introduction of thiophene-S,S-dioxides, is *not* paralleled by the increase in ionization potential and the induction of ambipolar charge transport properties, again in contrast with the introduction of thiophene-S,S-dioxides causing *n*-type charge transport. New limits of important properties can be attained such as reduction potentials on the order of -0.4 V, near the values of fullerene, and energy gaps in the order of 1.2 V. Moreover, new exciting fields of application can be foreseen. For example, taking into account that in thiophene-S-oxide the sulfur atom is pyramidal, it will be possible to design and synthesize configurationally stable building blocks for the preparation of

semiconducting chiral systems for chiral voltammetry[43] or innovative electronic devices such as spin-OLEDs that do not require magnetic elements to define the spin orientation.[44] Finally, the easy preparation of mono-oxygenated thiophene units allowed us to highlight - in the context of our previous biological applications of thiophene materials[14d] - the very different cytotoxicity of thiophene-S-oxides and thiophene-S,S-dioxides with regard to live cells, although both systems have the appropriate hydrophilicity/hydrophobicity balance to be spontaneously internalized by live cells. Even more important is the finding that the two systems display very different recognition capabilities for specific intracellular proteins through H bonding intermolecular interactions.

4. Experimental section

4.1. Synthesis and characterization. The synthesis of oxygenated thiophenes (Table 1) was performed in a FALC LBS1 50KHz Ultrasonic bath. Cross coupling reactions involving boron derivatives were carried out under microwave assistance in a Milestone Microsynth Labstation operating at 2450 MHz monitored by a proprietary control unit. All operations were carried out under a dry, oxygen-free nitrogen atmosphere. Organic solvents were dried by standard procedures. TLC was carried out with 0.2-mm thick of silica gel 60 F254 (Merck). Visualization was accomplished by UV light or phosphomolybdic acid solution. Preparative column chromatographies was performed on glass columns of different sizes hand packed with silica gel 60 (particle sizes 0.040-0.063 mm, Merck). H-1 and C-13 NMR spectra were recorded with a Varian Mercury-400 spectrometer equipped with a 5-mm probe. Chemical shifts were calibrated using the internal CDCl3 resonance which was referenced to TMS. Mass spectra were collected on a Thermo Scientific TRACE 1300 gas chromatograph. UV-Vis spectra were recorded using a Agilent Technologies CARY 100 UV-Vis spectrophotometer. Photoluminescence spectra were collected on a Perkin Elmer LS50 spectrofluorometer. The detailed preparation of all compounds and their characterization are reported in Supporting Information.

4.2. Cyclic Voltammetry. Solid state CVs were obtained employing an AMEL 5000 electrochemical cell under argon. Working electrodes were solid films of the oligomers or polymers deposited on ITO. An electrolytic solution of anhydrous propylene carbonate (Sigma-Aldrich) containing 0.1 mol L^{-1} tetraethylammonium tetrafloroborate (Fluka for electrochemical analysis) was used. The oxidation potential of ferrocene/ferricinium (Fc/Fc^{+} = -4.84 eV) *vs.* aqueous saturated calomel electrode (SCE) was 0.50 V. The CVs of 1 mmol L^{-1} oligomers were performed on Pt disc-electrode in DCM (Sigma-Aldrich, distilled on P_2O_5

and stored under Ar) 0.1 mmol L^{-1} tetrabutyl-ammonimum perchlorate (Fluka, recrystalized form methanol) where Fc/Fc^{+} = 0.47 V *vs.* SCE.

4.3. Single crystal X-Ray Diffraction. Crystallographic data collection and structure determination were performed with a single crystals of hexamer 1a5 grown from toluene. The X-ray intensity data of the compound were measured on a Bruker Apex II CCD diffractometer. Cell dimensions and the orientation matrix were initially determined from a least-squares refinement on reflections measured in three sets of 20 exposures, collected in three different ω regions, and eventually refined against all data. A full sphere of reciprocal space was scanned by 0.3° ω steps. The software SMART[45] was used for collecting frames of data, indexing reflections and determination of lattice parameters. The collected frames were then processed for integration by the SAINT program,[45] and an empirical absorption correction was applied using SADABS.[46] The structure was solved by direct methods (SIR 2004[47]) and subsequent Fourier syntheses and refined by full-matrix least-squares on F^2 (SHELXTL[48]) using anisotropic thermal parameters for all non-hydrogen atoms. All the hydrogen atoms were added in calculated positions, included in the final stage of refinement and refined with $U(H)=1.2U_{eq}(C)$ and allowed to ride on their carrier atoms. The oxygen atom of the sulphoxide group was found to be disordered over two sites with occupancy factor of 0.90 and 0.10, respectively. The SQUEEZE routine of the PLATON software[49] revealed that the structure contains solvent accessible voids (352$Å^3$/unit cell), filled with disordered solvent molecules (99 electrons/unit cell) that is most likely disordered toluene. Molecular graphics were generated by using Mercury 3.3.[50] Color codes for all molecular graphics: orange (Cu), blue (N), red (O), grey (C), white (H). Crystal data and details of data collections for compound A are reported in Table S4.

4.4 Field-effect transistors. Top-gate, staggered Field-Effect Transistors (FETs) operating both in *p*- and *n*- accumulation regimes were fabricated using polymers **1a1**, **1b1**, **5a2** as the active materials. Low alkali 1737F Corning glass was used as substrate, cleaned aequentially in an ultrasonic bath of deionized water, acetone and 2-propanol for 10 minutes each, then exposed to oxygen plasma at 100 W for 10 minutes. Bottom source and drain electrodes were defined by photolithography and evaporation of 1.5 nm of Cr and 25 nm of Au. The defined patterns feature a channel width W=10mm and channel length L=20μm or L=10 □m. Solutions of the three polymers with a concentration of 5 g/L in chloroform were prepared and deposited via spin-coating at 1000 rpm in nitrogen atmosphere, then the samples were annealed at 150 °C for 8 hours. Poly(methylmethacrylate), PMMA, was purchased from Sigma-Aldrich and dissolved in n-butyl acetate with a concentration of 80 g/L, then spin-

coated over the active material layer at 1500 rpm yielding a 500-nm-thick dielectric layer. The devices were then annealed at 80 °C for 30 mn. The gate electrodes were defined via evaporation of Al through a shadow mask. Electrical characterization was performed in a nitrogen atmosphere using an Agilent B1500A Semiconductor Parameter Analyzer.

4.5. Photoluminescence measurements in thin films. Emission spectra were obtained with an Edinburgh FLS980 spectrometer equipped with a peltier-cooled Hamamatsu R928 photomultiplier tube (185-850 nm). An Edinburgh Xe900 450 W Xenon arc lamp was used as exciting light source. Emission lifetimes in the ns-µs range were determined with the single photon counting technique by means of the same Edinburgh FLS980 spectrometer using a laser diode as excitation source (1 MHz, λexc = 407 nm, 200 ps time resolution after deconvolution) and the above-mentioned PMT as detector. Analysis of the luminescence decay profiles vs time was accomplished with the Decay Analysis Software provided by the manufacturer. Photoluminescence yields were calculated by corrected emission spectra obtained from an apparatus consisting of a barium sulphate coated integrating sphere (4 inches), a 450W Xe lamp (λexc = tunable by a monochromator supplied with the instrument) as light sources, and a R928 photomultiplayer tube as signal detectors, following the procedure described by De Mello et al.[51] Experimental uncertainties are estimated to be ± 8% for lifetime determinations, ± 20% for emission quantum yields, ± 2 nm and ± 5 nm for absorption and emission peaks, respectively. Absorption spectra were recorded with a Cary 5000 UV-Vis-Nir Varian spectrophotometer.

4.6. OLEDs fabrication and characterization. The OLEDs were fully fabricated by high vacuum thermal evaporation in a Kurt J. Lesker multiple high vacuum chamber system. The electrical-optical characteristics of the devices were measured under vacuum with an Optronics OL770 spectrometer, coupled, through an optical fiber, to the OL610 telescope unit for the luminance measurements, with an experimental uncertainty of around ± 10%. The whole system was National Institute of Standards and Technology (NIST) calibrated using a standard lamp and was directly connected by RS232 cable to a Keithley 2420 current-voltage source meter.

4.7. Cell viability. Mouse embryonic fibroblasts (NIH-3T3) were seeded at a density of 100,000 cells in tissue culture plate in 1 mL of complete culture medium. Compounds 5a1, 5b1, 5b2 were dissolved in the minimum amount of DMSO in order to obtain a stock solution and then were administered to the cells by adding the appropriate dilution in DMEM serum free to obtain the final concentration of 0.05 mg/mL and incubated at 37°C in 5% CO_2, 95% relative humidity for 1h. At the end of the incubation period, the cell cultures were repeatedly

washed with DMEM medium serum free. The cells were examined after 1, 24, 48, 72 hours and 7 days upon treatment by laser scanning confocal microscopy (LSCM). Confocal micrographs were taken with Leica confocal scanning system mounted into a Leica TCS SP5 (Leica Microsystem GmbH, Mannheim, Germany), equipped with a 63X oil immersion objective and spatial resolution of approximately 200 nm in x-y and 100 nm in z. After an appropriate incubation period, the cultures were removed from the incubator and the MTT (3-(4,5-dimethylthiazol-2-yl) -2,5-diphenyl tetra- zolium bromide) solution added in an amount equal to 10% of the culture volume. Then the cultures were returned to incubator and incubated for 3 hours. After the incubation period, the cultures were removed from the incubator and the resulting MTT formazan crystals were dissolved with acidified isopropanol solution to an equal culture volume. The plates were read within 1 hour after adding acidified isopropanol solution. The absorbance was spectrophotometrically measured at wavelength 570 nm and the background absorbance measured at 690 nm substracted. The percentage viability is expressed as the relative growth rate (RGR) by equation: RGR = (Dsample/ Dcontrol) *100% where Dsample and Dcontrol are the absorbances of the sample and the negative control.[24] Representative measurements of three distinct sets of data are reported (*Student t- test, $P < 0.05$*).

Supporting Information

Supporting Information is available from the Wiley Online Library or from the author.

Acknowledgements

Thanks are due do Dr. Massimo Gazzano (CNR-ISOF) for help in the preparation of the single crystal of hexamer **1a5**. This work was supported by the project *Molecular Nanotechnologies For Human Health and Environment* (PON R&C 611 2007-2013, code PON02_00563_3316357).

---

[1] a) H.D. Magurudeniya, P. Huang, S.S Gunathilake, E. A. Rainbolt, M. C. Biewer, M. C. Stefan, *Encyclopedia of Polymer Science and Technology*, **2014**, John Wiley & Sons, Inc., 1-36. b) T. P. Huynha, P. S. Sharma, M. Sosnowska, F. D'Souza, W. Kutnera, *Progress in Polymer Science* **2015**, *47*, 1-25. c) M. E. Cinar, T. Ozturk, *Chem. Rev.* **2015**, *115*, 3036-3140. d) L. Dou, Y. Liu, Z. Hong, G. Li, Y. Yang,

Chem. Rev. **2015**, *115*, 12633-12665. e) M. Iyoda, H. Shimizu, *Chem. Soc. Rev.* **2015**, ***44***, 6411-6424. f) S. C. Rasmussen, S. J. Evenson, C. B. McCausland, *Chem. Commun.* **2015**, *51*, 4528-4543. g) G. Barbarella, F. Di Maria, *Acc. Chem. Res.* **2015**, *48*, 2230-2241. h) J. A. Joule, Editor, *Thiophenes (Topics in Heterocyclic Chemistry)* **2015** Edition Springer International Publishing Switzerland. i) I. Perepichka, D. F. Perepichka, Eds., *Handbook of Thiophene-Based Materials: Applications in Organic Electronics and Photonics*, **2009**, John Wiley & Sons, Ltd.

[2] a) V. Malytskyi, J. J. Simon, L. Patrone, J. M. Raimundo, *RSC Adv.*, **2015**, *5*, 354-397. b) P. Qin, H. Kast, M. K. Nazeeruddin, S. M. Zakeeruddin, A. Mishra, P. Bäuerle, M. Grätzel, *Energy Environ. Sci.*, **2014**, *7*, 2981-2985.

[3] a) K. Takimiya, I. Osaka, I.; T. Mori, M. Nakano, *Acc. Chem. Res.*, **2014**, *47*, 1493-1502. b) R. S. Ashraf, A. J. Kronemeijer, *Chem. Commun*., **2012**, *48*, 3939-3941. c) A. Facchetti, *Chem. Mater*., **2011**, *23*, 733-758.

[4] a) L. B. G. Johansson, R. Simon, G. Bergström, M. Eriksson, S. Prokop, C. F. Mandenius, F. L. Heppner, F. L., A. K. O. Åslund, K. P. R. Nilsson, *Biosensors and Bioelectronics*, **2015**, *63*, 204-211. b) J. Ries, V. Udayar, A. Soragni, S. Hornemann, K. P. R. Nilsson, R. Riek, C. Hock, H. Ewers, A. A. Aguzzi, L. Rajendran, *ACS Chem. Neurosci.*, **2013**, *4*, 1057-1061.

[5] M. Dal Molin, Q. Verolet, A. Colom, R. Letrun, E. Derivery, M. Gonzalez-Gaitan, E. Vauthey, A. Roux, N. Sakai, S. Matile, *J. Am. Chem. Soc*., **2015**, *137*, 568-571.

[6] a) J. Nakayama, Y. Sugihara, *Sulfur Reports*, **1997**, *19*, 349-375. b) P. Pouzet, I. Erdelmeier, D. Ginderow, J. P. Mornon, P. Dansette, D. Mansuy, ***J. Chem. Soc., Chem. Commun.*, 1995**, 473-474. c) A. Bongini, G. Barbarella, M. Zambianchi, C. Arbizzani, M. Mastragostino, *Chem. Commun*., **2000**, 439-440. d) T. Thiemann, K. G. Dongol, *J. Chem. Research (M)*, **2002**, 0701–0719.

[7] a) J. Nakayama, H. Nagasawa, Y. Sugihara, A. Ishii, *J. Am. Chem. Soc*., **1997**, *119*, 9077-9078. b) J. Nakayama, *Sulfur Reports*, **2000**, *22*, 123-149. c) J. Nakayam, Y. Sano, Y. Sugihara, A. Ishii, *Tetrahedron Letters* **1999**, *40*, 3785-3788.

[8] A. Stoffregen, M. Heying, W. S. Jenks, , *J. Am. Chem. Soc.*, **2007**, *129*, 15746-15747.

[9] a) M. Moreno Oliva, J. Casado, J. T. LópezNavarrete, S. Patchkovskii, T. Goodson III, M. R. Harpham, J. S. Seixas deMelo, E. Amir, S. Rozen, *J. Am. Chem. Soc*., **2010**, *132*, 6231-6242. b) G. Barbarella, L. Favaretto, M. Zambianchi, O. Pudova, C. Arbizzani, A. Bongini, M. Mastragostino, *Adv. Mater.*, **1998**, *10*,

551-554. c) G. Barbarella, L. Favaretto, G. Sotgiu, M. Zambianchi, L. Antolini, O. Pudova, A. Bongini, *J.Org.Chem*. **1998**, *63*, 5497-5506. d) L. Antolini, E. Tedesco, G. Barbarella, L. Favaretto, G. Sotgiu, M. Zambianchi, D. Casarini, G. Gigli, R. Cingolani, *J. Am. Chem. Soc.*, **2000**, *122*, 9006-9013. e) A. Bongini, G. Barbarella, M. Zambianchi, C. Arbizzani , M. Mastragostino, *Chem. Commun.*, **2000**, 439-440.

[10] a) J. Biwang, T. D. Tilley, *J. Am. Chem. Soc.*, **1999**, *121*, 9744-9745. b) M. C. Su, J. Biwang J., T. D. Tilley, *Angew. Chem. Int. Ed.*, **2000**, *39*, 2870-2873.

[11] a) S. Rozen, Y. Bareket, *J. Org. Chem,*. **1997**, *62*, 1457-1462. b) E. Amir, S. Rozen, *Angew. Chem. Int. Ed.*, **2005**, *44*, 7374-7378. c) N. Shefer, T. Harel, S. Rozen, *J. Org. Chem.*, **2009**, *74*, 6993-6998. d) S. Rozen, *Acc. Chem. Res,*. **2014**, *47*, 2378-2389.

[12] a) E. J. Dell, B. Capozzi, J. Xia, L. Venkataraman, L. M. Campos, *Nat. Chem.*, **2015**, *7*, 209-214. b) E. Busby, J. Xia, Q. Wu, J. Z. Low, R. Song, J. R. Miller, X. Y. Zhu, L. M. Campos, M. Y. Sfeir, *Nat. Mater.*, **2015**, *14*, 426-433. c) B. Capozzi, J. Xia, O. Adak, E. J. Dell, Z. F. Liu, J. C. Taylor, J. B. Neaton, L. M. Campos, L. Venkataraman, *Nat. Nanotechnol*., **2015**, *10*, 522-527. d) E. J. Dell, Campos, L. M. *J. Mater. Chem.*, **2012**, *22*, 12945-12952.

[13] N. Ghofraniha, I. Viola, F. Di Maria, G. Barbarella, G. Gigli, L. Leuzzi, C. Conti, *Nat. Commun*., **2015**, *6*, article 6058.

[14] a) G. Barbarella, F. Di Maria, *Acc. Chem. Res.*, **2015**, *48*, 2230-2241. b) I. E. Palamà, F. Di Maria, S. D'Amone, G. Barbarella, G. Gigli, *J. Mater. Chem. B* **2015**, *3*, 151-158. c) P. Ji, X. Xu, S. Ma, J. Fan, Q. Zhou, X. Mao, C. Qiao, **2015**, *6*, 1010-1014. d) I. E. Palamà, F. Di Maria, I. Viola, E. Fabiano, G. Gigli, C. Bettini, G. Barbarella, *J. Am. Chem. Soc.*, **2011**, *133*, 17777–17785.

[15] C. Santato, L. Favaretto, M. Melucci, A. Zanelli, M. Gazzano, M. Monari, D. Isik, D. Banville, S. Bertolazzi, S. Loranger, F. Cicoira, *J.Mater.Chem.*, **2010**, *20*, 669-676.

[16] a) J. Lindley, T. Mason, *J. Chem. Soc. Rev.*, **1987**,*16*, 275-311. b) P. Arsenyan, E. Paegle, S. Belyakov, *Tetrahedron Lett.*, **2010**, *51*, 205-208.

[17] P. Pouzet, P. I. Erdelmeier, D. Ginderow, J. P. Mornon, P. Dansette, D. Mansuy, *J. Chem. Soc., Chem. Commun,*. **1995**, 473-474.

[18] G. Barbarella, L. Favaretto, G. Sotgiu, M. Zambianchi, C. Arbizzani, A. Bongini, A.; M. Mastragostino, *Chem.Mater.*, **1999**, *11*, 2533-2541.

[19] S. Raasch, in *Chemistry of Heterocyclic Compounds, Thiophene and its Derivatives*, ed. S. Gronowitz, Wiley, New York, **1985**, *44*, 871.

[20] S. Rozen, Y. Bareket, *J. Org. Chem.*, **1997**, *62*, 1457-1462.

[21] C. C. C. Johansson Seechurn, M. O., Kitching, T. J. Colacot, V. Snieckus, *Angew. Chem. Int. Ed.*, **2012**, *51*, 5062-5085.

[22] G. Barbarella , L. Favaretto, A. Zanelli, G. Gigli, M. Mazzeo, M. Anni, A. Bongini, *Adv. Funct. Mater.*, **2005**, *15*, **664-670.**

[23] E. Lukevics, P. Arsenyan, S. Belyakov, O. Pudova, *Chem. Heterocycl. Comp.*, **2002**, *38*, 632-645.

[24] T. M. Pappenfus, J. H. Melby, B. B. Hansen, D. M. Sumption, S. A. Hubers, D. E. Janzen, P. C. Eubank, K. A. McGee, M. W. Burand, K. R. Mann, *Org. Lett.*, **2007**, *9*, 3721-3724.

[25] a) C. M. Cardona, W. Li, A. E. Kaifer, D. Stockdale, G. C. Bazan, *Adv. Mater.*, **2011**, *23*, 2367-2371. b) S.Trasatti, *Pure Appl. Chem.*, **1986**, *58*, 955-966. c) G. Gratzner, J. Kuta, *Pure Appl. Chem.*, **1984**, *56*, 461-466.

[26] E. Bundgaard, F. C. Krebs, *Sol. Energ. Mat. Sol. C.*, **2007**, *91*, 954985.

[27] a) L. Echegoyen, L. E. Echegoyen, L. E. *Acc. Chem. Res.*, **1998**, *31*, 593-601. b) P. Damlin, M. Hätönen, S. E. Domínguez, T. Ääritalo, T.; H. Kivelä, C. Kvarnström, *RSC Adv.*, **2014**, *4*, 8391-8401.

[28] E. Busby, J. Xia, J. Z. Low, Q. Wu, J. Hoy, L. M. Campos, M. Y. Sfeir, *J. Phys. Chem. B,* **2015**, *119*, 7644-7650.

[29] M. A. Baldo, S. Lamansky, P. E. Burrows, M. E. Thompson, S. R. Forrest, *Appl. Phys. Lett.* **1999**, *75*, 4-6.

[30] J. Kalinowski, W. Stampor, M. Cocchi, D. Virgili, V. Fattori, P. Di Marco, *Chem. Phys.* **2004**, *297*, 39-48.

[31] D. Natali, M. Caironi, *Adv. Mater.*, **2012**, *24*, 1357-1387.

[32] H. Sirringhaus, *Adv.Mater.* **2005**, *17*,2411-2425.

[33] a) J. E. Cochran, E. Amir, K. Sivanandan, S. Y. Ku, J. H. Seo, B. A. Collins, J. R. Tumbleston, M. F. Toney, H. Ade, C. J. Hawker, M. L Chabiny, *J. Polym. Sci., Part B: Polym. Phys.*, **2013**, *51*, 48-56. b) Y. R. Shin, W. H. Lee, J. B. Park, H. Kim, S. K. Lee, W. S. Shin, D. H. Hwang, I. N. Kang., *J. Pol. Sci Part A: Pol. Chem.*, **2015**, DOI: 10.1002/pola.27797.

[34] a) A. R. Murphy, J. M. J. Fréchet, *Chem.Rev.*, **2007**, *107*, 1066-1096. b) A. Facchetti, *Chem. Mater*., **2011**, *23*, 733-758.

[35] L. L. Chua, J. Zaumseil, J. F. Chang, E. C. W. Ou, P. K. H. Ho, H. Sirringhaus, R. H. Friend, R. H. *Nature*, **2005**, *434*, 194-199.

[36] L. Antolini, E. Tedesco, G. Barbarella, L. Favaretto, G. Sotgiu, M. Zambianchi, D. Casarini, G. Gigli, R. Cingolani, *J.Am.Chem.Soc.* **2000**, *122*, 9006-9013.

[37] a) E. Amir, K. Sivanandan, A. Cochran, A. *Polym Chem.*, **2011**, *49*, 1933-1941. b) M. Pasini, S. Destri, W. Porzio, C. Botta, U. Giovanella, *J. Mater. Chem.*, **2003**, *13*, 807-813.

[38] L. Favaretto, G. Barbarella, I. Rãu, F. Kajzar, S. Caria, M. Murgia, R. Zamboni, *Optics Express*, **2009**, *17*, 2557-2564.

[39] F. B. Dias, K. N. Bourdakos , V. Jankus, K. C. Moss, K. T. Kamtekar, V. Bhalla, J. Santos, M. R. Bryce, A. P. Monkman, *Adv. Mater*,. **2013**, *25*, 3707-3714.

[40] F. Denizot, R. Lang, *J. Immunol. Methods*, **1986**, *89*, 271-277.

[41] a) L A. Constantin, E. Fabiano, F. Della Sala, *Phys. Rev.*, *B* **2012**, *86*, 035130. b) L. A. Constantin, E. Fabiano, F. Della Sala, *J. Chem. Theory Comput*., **2013**, *9*, 2256-2263. c) L. A. Constantin, E. Fabiano, F. Della Sala, *Phys. Rev. B*, **2013**, *88*, 125112.

[42] a) J. Contreras-Garcia, E. R. Johnson, S. Keinan, R. Chaudret, J. P. Piquemal, D. N. Beratan, W. Yang, *J. Chem. Theory Comput.*, **2011**, *7*, 625-632. b) J. Contreras-Garcia, W. Yang, E. R. Johnson, *J. Phys. Chem.*, *A* **2011**, *115*, 12983-12990.

[43] P. C. Mondal, N. Kantor-Uriel, S. P. Mathew, F. Tassinari, C. Fontanesi, R. Naaman, *Adv. Mater.*, **2015**, *27*, 1924-1927.

[44] a) S. Arnaboldi, T. Benincori, R. Cirilli, W. Kutner, M. Magni, P. R. Mussini, K. Noworyta, F. Sannicolò, F. *Chem. Sci.*, **2015**, *6*,1706-1711. b) F. Sannicolò, S. Arnaboldi, T. Benincori, V. Bonometti, R. Cirilli, L. Dunsch, W. Kutner, G. Longhi, P. R. Mussini, M. Panigati, M. Pierini, S. Rizzo, *Angew. Chem. Int. Ed.*, **2014**, 53, 2623-2627.

[45] SMART & SAINT Software Reference Manuals, version 5.051 (Windows NT Version), Bruker Analytical X-ray Instruments Inc.: Madison, WI, **1998**.

[46] Sheldrick, G. M. SADABS, program for empirical absorption correction, University of Göttingen, Germany, **1996**.

[47] M. C. Burla, R. Caliandro, M. Camalli, B. Carrozzini, G. L. Cascarano, L. De Caro, C. Giacovazzo, C.; Polidori, G.; Spagna, R. *J. Appl. Crystallogr.* **2005**, *38*, 381-388.

[48] Sheldrick, G. M. SHELXTLplus (Windows NT Version) Structure Determination Package, Version 5.1. Bruker Analytical X-ray Instruments Inc.: Madison, WI, USA, **1998**.

[49] A. L. Spek, *Acta Crystallogr.*, **2009**, *D65*, 148-155.

[50] C. F. Macrae, I. J. Bruno, J. A. Chisholm, P. R. Edgington, P. McCabe, E. Pidcock, L. Rodriguez-Monge, R. Taylor, J. van de Streek, P. A. Wood, *J. Appl. Crystallogr.*, **2008**, *41*, 466-470.

[51] J. C. De Mello, F. Wittmann, R. H. Friend, *Adv. Mater.*, **1997**, *9*, 230-232.